

## Effect of Graded Double Perovskite for Boosting up the Photovoltaic Output Parameters of Solar Cell: A Numerical Modelling Using SCAPS-1D

A. Yousfi\*, W. Feneniche

ETA Laboratory, Electronics Department, University Mohamed El Bachir El Ibrahimi of Bordj Bou Arréridj, 34000, Algeria

(Received 15 August 2023; revised manuscript received 18 December 2023; published online 27 December 2023)

Recently, extensive researches focus on the development of solar cells based on new absorber materials, perovskite is one of these key candidates for solar cells applications, according to its good results in the output parameters which is confirmed by the photovoltaic community. In this work we will investigate, simulate numerically via SCAPS-1D and compare the structure of graded double perovskite based on MAPbI<sub>3</sub>/LNMO with the conventional recent one. We use the absorbers of MAPbI<sub>3</sub> and LNMO as sandwich between the materials ETL of ZnO and HTL of Cu<sub>2</sub>O to simulate the proposed structure. The developed device shows a good enhanced power conversion efficiency of 24.01 %.

**Keywords:** Perovskite, MAPbI<sub>3</sub>,  $J_{sc}$ ,  $V_{oc}$ , PCE, Work Function, SCAPS-1D.

DOI: [10.21272/jnep.15\(6\).06002](https://doi.org/10.21272/jnep.15(6).06002)

PACS numbers: 88.40.jm, 85.60. – q

### 1. INTRODUCTION

The photovoltaic solar cells have a tremendous development in the last few years, according to the inserting of perovskite materials to adjust and increasing the efficiency of the solar cell. The use of the absorber layer of perovskite based on methylammonium lead iodide (MAPbI<sub>3</sub>) which play a great role in the way of giving the conventional device better performances, according to the admirable absorption, lesser energy of exciton-binding, large charge carrier mobility, tunable optical bandgap, and lesser temperature of working than other solar cells [1-3]. Not so far, solar cells based on perovskite achieve a very good efficiency of 25.2% which turn it or class it as a cheap device [4-8].

Nevertheless, toxicity in solar cells based on perovskite absorber considered as a major problem related to the lead Pb, in this work we will see the important of the output parameters for the double graded absorber MAPbI<sub>3</sub>/LNMO, our target is to make under investigation the graded double perovskite solar cell of the structure, FTO/ZnO/MAPbI<sub>3</sub>/LNMO/Cu<sub>2</sub>O/Au. In the way of increasing the output photovoltaic parameters such as:  $J_{sc}$ ,  $V_{oc}$ , FF and PCE. The SCAPS-1D software simulator used to verify, modify and enhance the current structure by exploiting input parameters such as thicknesses, doping concentration acceptors or donors, defect density, ETLs, HTLs and we finalize our investigation via the use of the appropriate back work function.

### 2. SIMULATED DEVICE STRUCTURES

Under an extern illumination of AM1.5 G at a temperature of 300 K, a numerical modelling is done using the solar cell capacitance simulator (SCAPS-1D), which is developed by Burgelman et al at university of Gent in Belgium. We should know that SCAPS-1D has a limit of the number of layers at 7 layers at maximum, the equations of Poisson and continuity are integrated to calculate the output parameters in SCAPS-1D [9-16]. The proposed configuration of FTO/ZnO/MAPbI<sub>3</sub>/LNMO/Cu<sub>2</sub>O/Au is developed as

illustrated in Fig. 1, accompanied with its energy band mechanism which explains the movement of electrons from absorber to the front contact and the holes from absorber to the back contact too. The structure parameters are presented in Table 1. Nevertheless, the working mechanism used in the developed device presented in Fig. 1b, shows the collections and movement of electrons and holes from the absorber into the front and back contact. Table 1 lists the input photovoltaic parameters using in the current development.

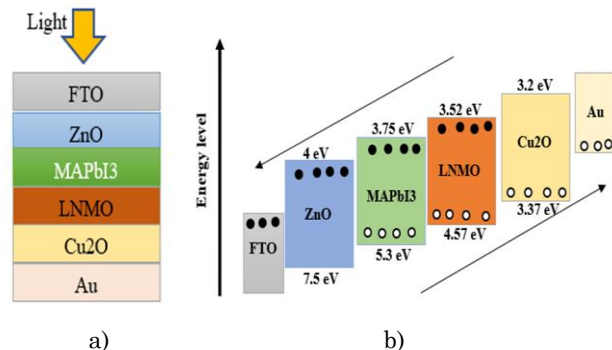


**Fig. 1** – Presents successively (a) the structure of FTO/ZnO/CH<sub>3</sub>NH<sub>3</sub>PbI<sub>3</sub>/LNMO/Cu<sub>2</sub>O/Au and (b) Energy band diagram at the illuminance of AM1.5 G

As illustrated in Fig. 2, the  $I(V)$  characteristics of the proposed configuration functions of different ETLs which gives the possibility to select the suitable one for the used structure, we noticed that the ZnO material considered as a good candidate comparing with C<sub>60</sub>, TiO<sub>2</sub> and SnS<sub>2</sub>.

The quantum efficiency presented in the Fig. 3 functions of wavelength from 300 to 900 nm present a better value for the candidate ZnO and SnS<sub>2</sub> which make the used structure more suitable and promising than the rest materials of C<sub>60</sub> and TiO<sub>2</sub>.

\* [abderrahim.yousfi@univ-bba.dz](mailto:abderrahim.yousfi@univ-bba.dz)

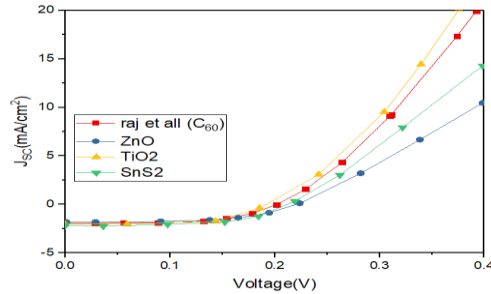


Fig. 2 – Present Current-Voltage characteristics for different ETLs

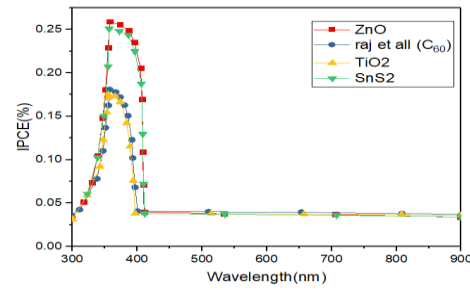


Fig. 3 – Illustrated QE versus Wavelength for different ETLs

Table 1 – Simulation of the input parameters of the device configuration

Material properties	FTO	TiO <sub>2</sub>	MAPbI <sub>3</sub>	LNMO	Cu <sub>2</sub> O
Thickness, $d$ (nm)	500	100	800	350	200
Electron Affinity, $\chi$ (eV)	4	3.9	3.75	3.32	3.2
Band gap, $Eg$ (eV)	3.5	3.2	1.55	1.05	2.17
Relative Permittivity, $\epsilon_r$	9	32	6.5	3.5	7.11
Effective Density of States (CB) $N_C$ (cm <sup>-3</sup> )	$2.2 \times 10^{18}$	$2.2 \times 10^{18}$	$2.2 \times 10^{15}$	$10^{18}$	$2 \times 10^{17}$
Effective Density of States (VB) $N_V$ (cm <sup>-3</sup> )	$1.8 \times 10^{19}$	$2.2 \times 10^{18}$	$2.2 \times 10^{17}$	$1 \times 10^{19}$	$1.1 \times 10^{19}$
Electron Mobility, $\mu_n$ (cm <sup>2</sup> /Vs)	20	20	200	22	20
Hole Mobility, $\mu_p$ (cm <sup>2</sup> /Vs)	10	10	20	22	80
Acceptor Density, $N_A$ (cm <sup>-3</sup> )	5	5	$1 \times 10^{13}$	$7 \times 10^{16}$	$10^{18}$
Donor Density, $N_D$ (cm <sup>-3</sup> )	$10^{19}$	$10^{17}$	$1 \times 10^{16}$	5	$10^7$
Defect Density, $N_t$ (cm <sup>-3</sup> )	$10^{14}$	$10^{14}$	$10^{14}$	$10^{14}$	$10^{14}$
References	[17]	[18]	[19]	[20]	[21,22]

Table 2 – Contains the different ETLs materials used to optimize the developed simulated device

Material properties	SnS <sub>2</sub>	C <sub>60</sub>	ZnO
Thickness, $d$ (nm)	100	100	100
Electron Affinity, $\chi$ (eV)	4.24	3.9	4
Band gap, $Eg$ (eV)	2.24	1.7	3.4
Relative Permittivity, $\epsilon_r$	10	4.2	9
Effective Density of States (CB) $N_C$ (cm <sup>-3</sup> )	$2.2 \times 10^{18}$	$8 \times 10^{19}$	$10^{18}$
Effective Density of States (VB) $N_V$ (cm <sup>-3</sup> )	$1.8 \times 10^{19}$	$8 \times 10^{19}$	$2 \times 10^{20}$
Electron Mobility, $\mu_n$ (cm <sup>2</sup> /Vs)	50	100	100
Hole Mobility, $\mu_p$ (cm <sup>2</sup> /Vs)	50	$3.5 \times 10^{-3}$	25
Acceptor Density $N_A$ (cm <sup>-3</sup> )	5	1	5
Donor Density $N_D$ (cm <sup>-3</sup> )	$10^{17}$	$2.6 \times 10^{18}$	$1 \times 10^{16}$
Defect Density $N_t$ (cm <sup>-3</sup> )	$10^{14}$	$10^{14}$	$10^{14}$
References	[23]	[20]	[24,25]

## 2.1 The impact of LNMO thickness on $J_{SC}$ , $V_{OC}$ , FF, and PCE

In this part, we study the variation of output photovoltaic parameters functions of thickness of the absorber LNMO from 200 nm to 1000 nm, the short circuit current has its optimal value of 2.05 mA in the thickness of 400 nm, the open circuit voltage has in the same point of thickness 0.23 V, we noticed that the used structure works at 400 nm also for the fill factor of 50.04 % and power conversion efficiency of 24.01 %.

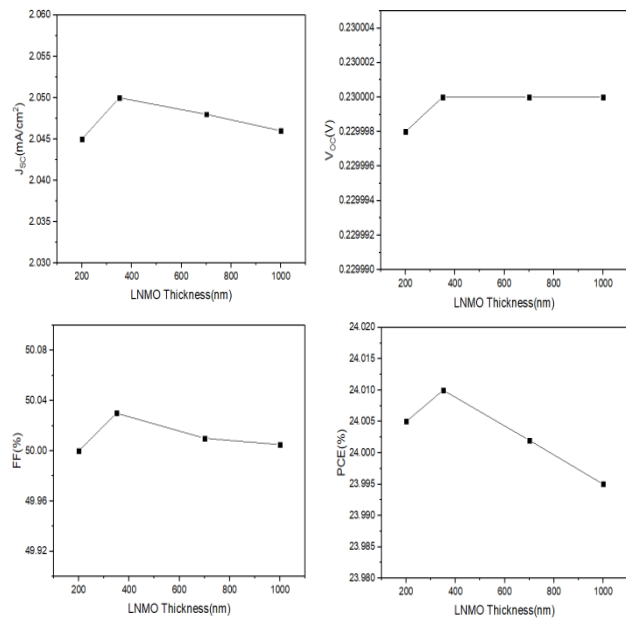


Fig. 4 – Variation of output parameters versus LNMO thickness

## 2.2 The Impact of $\text{MAPbI}_3$ Thickness on $J_{\text{sc}}$ , $V_{\text{oc}}$ , FF, and PCE

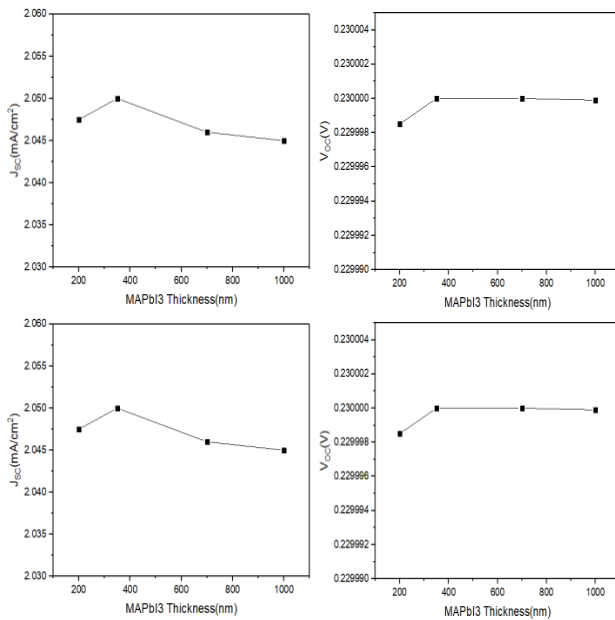


Fig. 5 – Variation of output parameters versus  $\text{MAPbI}_3$  thickness

The second part of optimization by varying the thickness of absorber layer of  $\text{MAPbI}_3$ , we have noticed that the output parameters very lightly comparing to the previous part of absorber.

## 2.3 The Influence of Back Work Function on the Output Photovoltaic Parameters Such as: $J_{\text{sc}}$ , $V_{\text{oc}}$ , FF, and PCE

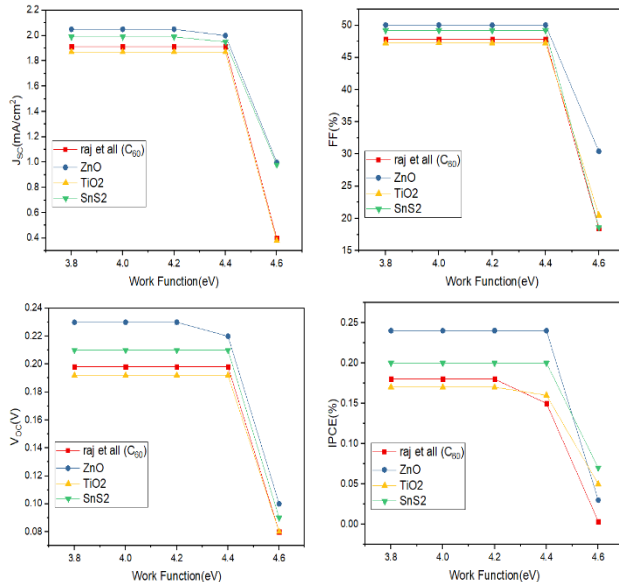


Fig. 6 – Output parameters functions of work function of the front contact

## REFERENCES

1. J.F. Liao, W.Q. Wu, Y. Jiang, D.B. Kuang, L. Wang, *Sol. RRL*, **3** No 3, 1800268 (2019).
2. T. Wang, D. Ding, X. Wang, R. Zeng, H. Liu, W. Shen, *ACS Omega* **3** No 12, 18434 (2018).
3. F. Zhang, X. Yang, H. Wang, M. Cheng, J. Zhao, L. Sun, *ACS Appl. Mater. Interfaces* **6** No 18, 16140 (2014).
4. NREL, Accessed. 10.4.2020, <https://www.nrel.gov/pv/cell-efficiency.html>.

In this part, we see the variation of work function versus the output parameters of the current configuration. The obtained results ranged from 3.8 eV to 4.2 eV are in good values such as  $J_{\text{sc}} = 2.05$  ( $\text{mA}/\text{cm}^2$ ),  $V_{\text{oc}} = 0.23$  V,  $FF = 50.03$  % and  $PCE = 24.01$  %, and more than 4.2 eV the parameters down, also at 4.6 eV down more and more.

Table 3 – Summarizes the results of the two simulated configurations

Configuration	$J_{\text{sc}}$ ( $\text{mA}/\text{cm}^2$ )	$V_{\text{oc}}$ (V)	FF (%)	PCE (%)
Raj et al [20] (C <sub>60</sub> /LNMO/CuI)	1.911	0.1982	47.82	18
Present simulation (ZnO/MAPbI <sub>3</sub> /LM O/Cu <sub>2</sub> O)	2.05	0.23	50.03	24.01

## 3. CONCLUSION

In this investigation, promising results were obtained through the use of the graded double perovskite  $\text{MAPbI}_3/\text{LNMO}$  and show their effect on the photovoltaic output parameters. A variety of numerous calculations were performed by using different material of electron transport layer as  $\text{SnS}_2$ ,  $\text{TiO}_2$ ,  $\text{C}_{60}$  and  $\text{ZnO}$ , and we conclude that  $\text{ZnO}$  is the suitable candidate in the current structure of  $\text{FTO/ZnO/MAPbI}_3/\text{LNMO/Cu}_2\text{O/Au}$ , the impact of work function also has a good effect on the device which leads the electrons and holes move rapidly from absorber to front and back contacts according to a specific transport mechanisms, the output parameters are in good way when the back contact are down ranged from 3.8 to 4.2 eV. The results values obtained in this simulation are,  $J_{\text{sc}} = 2.05 \text{ mA}/\text{cm}^2$ ,  $V_{\text{oc}} = 0.23$  V,  $FF = 50.03$  % and  $PCE = 24.01$  %.

## AKNOWLEDGEMENTS

Special thanks to the team of Mr. Marc Burgelman (from the university of Gent-Belgium) for facilitate using SCAPS-1D, and also for the Editor-in-Chief of the Journal of Nano- and Electronic Physics.

5. W.S. Yang, B.W. Park, E.H. Jung, N.J. Jeon, Y.C. Kim, D.U. Lee, S.S. Shin, J. Seo, E.K. Kim, J.H. Noh, S.I. Seok, *Science* **356** No 6345, 1376 (2014).
6. J.P. CorreaBaena, A. Abate, M. Saliba, W. Tress, T.J. Jacobss, M. Grätzel, A. Hagfeldt, *Energy Environ. Sci.* **10** No 3, 710 (2017).
7. M. Saliba, T. Matsui, J.Y. Seo, K. Domanski, J.P. CorreaBaena, M.K. Nazeeruddin, S.M. Zakeeruddin, W. Tress, A. Abate, A. Hagfeldt, M. Grätzel, *Energy Environ. Sci.* **9** No 6, 1989 (2016).
8. L.K. Ono, E.J. JuarezPerez, Y. Qi, *ACS Appl. Mater. Interfaces* **9** No 36, 30197 (2017).
9. M. Burgelman, P. Nollet, S. Degrave, *Thin Solid Film*, **361-362** No 3, 527 (2000).
10. F. Liu, J. Zhu, J. Wei, Y. Li, M. Lv, S. Yang, B. Zhang, J. Yao, S. Dai, *Appl. Phys. Lett.* **104** No 25, 253508 (2014).
11. P. Lin, K. Tan, J. Tan, L. Wu, G. Wang, S. Jin, Y. Lin, In *Proceedings of the 31st European Photovoltaic Solar Energy Conference and Exhibition* (Hamburg, Germany).
12. A. Baktash, O. Amiri, A. Sasani, *Superlattice. Microstruct.* **93**, 128 (2016).
13. K. Sobayel, M. Akhtaruzzaman, K.S. Rahman, M.T. Ferdaous, Z.A. AlMutairi, H.F. Alharbi, N.H. Alharthi, M.R. Karim, S. Hasmady, N. Amin, *Res. Phys.* **12**, 1097 (2019).
14. K. Sobayel, M. Shahinuzzaman, N. Amin, M.R. Karim, M.A. Dar, R. Gul, M.A. Alghoul, K. Sopian, A.K.M. Hasan, M. Akhtaruzzaman, *Sol. Energy* **207** No 3, 479 (2020).
15. S. Mahjabin, M.M. Haque, K. Sobayel, M.S. Jamal, M.A. Islam, V. Selvanathan, A.K. Abdulaziz, H.F. Alharbi, K. Sopian, N. Amin, M. Akhtaruzzaman, *IEEE Access* **20**, 106346 (2020).
16. K. Sobayel, K.S. Rahman, M.R. Karim, M.O. Aijaz, M.A. Dar, M.A. Shar, H. Misran, N. Amin, *Chalcogenide Lett.* **15**, 105478299 (2018).
17. M.F.M. Noh, C.H. Teh, R. Daik, E.L. Lim, C.C. Yap, M.A. Ibrahim, N.A. Ludin, A.R.B.M. Yusoff, J. Jang, M.A.M. Teridi, *J. Mater. Chem. C* **6** No 4, 2050 (2018).
18. F. Hao, C.C. Stoumpos, D.H. Cao, R.P.H. Chang, M.G. Kanatzidis, *Nat. Photon.* **8** No 489-494, 1749, (2014).
19. A.S. Chouhan, N.P. Jasti, S. Avasthi, *Mater. Lett.* **221**, 167 (2018).
20. A. Raj, A. Anshul, V. Tuli, P.K. Singh, R.C. Singh, M. Kumar, *Mater. Today: Proc.* **47**, 1656 (2021).
21. M. Shasti, A. Mortezaali, *phys. status solidi a* **216** No 18, 1862 (2019).
22. P.K. Patel, *Sci. Rep.* **11** No 1, 2045 (2021).
23. Shyma, Arunkumar Prabhakaran et Sellappan, Raja, *Materials* **15** No 21, 7859 (2022).
24. N. Lakhdar, A. Hima, *Opt. Mater.* **99** No 109517, 925 (2019).
25. F. Azri, A. Meftah, N. Sengouga, A. Meftah, *Sol. Energy* **181**, 38 (2019).

## Вплив градуйованого подвійного перовскіту для підвищення фотоелектричних вихідних параметрів сонячної батареї: чисельне моделювання за допомогою SCAPS-1D

A. Yousfi, W. Feneniche

*ETA Laboratory, Electronics Department, University Mohamed El Bachir El Ibrahimi of Bordj Bou Arréridj, 34000, Algeria*

Останнім часом значні дослідження зосереджені на розробці сонячних елементів на основі нових поглинаючих матеріалів. Перовскіт є одним із цих ключових матеріалів для застосування в сонячних елементах через його гарні результати у вихідних параметрах, що підтверджено фотоелектричними властивостями. У цій роботі було досліджене та чисельно змодельовано за допомогою SCAPS-1D і проведено порівняння структури градуйованого подвійного перовскіту на основі  $\text{MAPbI}_3/\text{LNMO}$  зі звичайною структурою. Були використані поглиначі  $\text{MAPbI}_3$  і  $\text{LNMO}$  як подвійний шар між матеріалами ETL  $\text{ZnO}$  і HTL  $\text{Cu}_2\text{O}$  для моделювання запропонованої структури. Розроблений пристрій показує хороший підвищений КЕД перетворення електроенергії на рівні 24,01 %.

**Ключові слова:** Перовскіт,  $\text{MAPbI}_3$ ,  $J_{sc}$ , Voc, PCE, Робоча функція, SCAPS-1D.